2-Aminophenoxazine-3-one-induced apoptosis via generation of reactive oxygen species followed by c-jun N-terminal kinase activation in the human glioblastoma cell line LN229

XIAO-FANG CHE[1], SHOTA MORIYA[1], CHUN-LEI ZHENG[2], AKIHISA ABE[1], AKIO TOMODA[1] and KEISUKE MIYAZAWA[1]

[1]Department of Biochemistry, Tokyo Medical University, Shinjuku-ku, Tokyo 160-8402, Japan; [2]Department of Medical Oncology, Cancer Hospital, Fudan University, Shanghai 200032, P.R. China

Received July 4, 2013; Accepted August 2, 2013

DOI: 10.3892/ijo.2013.2088

Abstract. 2-Aminophenoxazine-3-one (Phx-3) induces apoptosis in several types of cancer cell lines. However, the mechanism of apoptosis induction by Phx-3 has not been fully elucidated. In this study, we investigated the anticancer effects of Phx-3 in the glioblastoma cell line LN229 and analyzed its molecular mechanism. The results indicated that 6- and 20-h treatment with Phx-3 significantly induced apoptosis in LN229 cells, with downregulation of survivin and XIAP. Both ERK and JNK, which are the members of the MAPK family, were activated after treatment with Phx-3. Inhibition of ERK using the specific inhibitor U0126 blocked the Phx-3-induced apoptosis only in part. However, inhibition of JNK using the specific inhibitor SP600125 completely prevented Phx-3-induced apoptosis and restored the phosphorylation states of ERK to the control levels. Enhanced generation of reactive oxygen species (ROS) was detected after 3-h treatment with Phx-3. In addition, the ROS scavenger melatonin almost completely blocked Phx-3-induced JNK activation and apoptosis. This suggests that JNK activation was mediated by Phx-3-induced ROS generation. Although SP600125 and melatonin completely blocked the reduction of mitochondrial membrane potential after a 3-h treatment with Phx-3, extension of Phx-3 exposure time to 20 h resulted in no cancelation of mitochondrial depolarization by these reagents. These reagents also had little effect on the decreased expression of survivin and XIAP during a 3-20-h exposure to Phx-3. These results indicate that the production of ROS following JNK activation is the main axis of Phx-3-induced apoptosis in LN229 cells for short-term exposure to Phx-3, whereas alternative mechanism(s) appear to be involved in apoptosis induction during long-term exposure to Phx-3.

Correspondence to: Dr Keisuke Miyazawa, Department of Biochemistry, Tokyo Medical University, 6-1-1 Shinjuku, Shinjuku-ku, Tokyo 160-8402, Japan
E-mail: miyazawa@tokyo-med.ac.jp

Key words: 2-aminophenoxazine-3-one, JNK, ROS, apoptosis

Introduction

Glioblastoma is the most common type of aggressive brain tumor in adults, with a poor prognosis. Chemotherapy is often performed in addition to radiation therapy as an adjuvant therapy for glioblastoma. However, a major obstacle for successful treatment is that it is difficult for chemotherapeutic agents to cross the blood-brain barrier to achieve sufficient concentrations (1).

Most chemically synthesized phenoxazines, which are the reductive form, are hardly soluble in water and exert little anticancer effect. However, some oxidative forms of phenoxazines [e.g., 2-aminophenoxazine-3-one (Phx-3)], which is synthesized by the biological reactions of *o*-aminophenol with bovine hemoglobin solution or bovine erythrocytes (2,3), exhibit anticancer activity *in vitro* and *in vivo* (4-10). Phx-3 inhibits cell growth and induces apoptosis in various cancer cell lines *in vitro* (5,6,8). Phx-3 also suppresses the growth of mouse malignant melanoma B16 cells transplanted in mice (7). Azuine *et al* reported that phenoxazine derivatives can pass through the blood-brain barrier (11). Because of this feature, Phx-3 is a potential anticancer agent for glioblastoma; however, its effect on glioblastoma has not been well characterized.

Regarding cellular fate in response to cell damage, commitment to apoptosis or evasion of apoptosis is determined by the balance of the complex survival-and-death signaling network. Various cell growth factors [e.g., epidermal growth factor receptor (EGFR), platelet-derived growth factor (PDGF), basic fibroblast growth factor (bFGF), transforming growth factor (TGF)-β and insulin-like growth factor (IGF)-1)] are overexpressed and activated in glioblastoma cells and thus are advantageous for oncogenesis (12). In the growth factor receptor signaling transduction, the most important pathways involved in oncogenesis are the phosphatidylinositide 3-kinases (PI3K)/Akt and Ras/MEK/ERK pathways (13). Akt, the central node in the complex cascade of PI3K signaling, is activated in various tumors, including glioblastoma and is

involved in cell survival and proliferation as well as the anti-apoptotic effect (14). Extracellular signal-regulated kinase (ERK) activation is generally associated with cell survival, proliferation and death. Some studies suggest that the balance between the intensity and the duration of pro- versus anti-apoptotic signals transmitted by ERK determines whether the cell undergoes proliferation or apoptosis (15). In addition, c-jun N-terminal kinase (JNK), another subgroup of the mitogen-activated protein kinase (MAPK) family, has been implicated in pro-apoptotic signaling and is activated by many types of stress (e.g., UV irradiation, inhibition of protein synthesis and exposure to anticancer reagents) (16).

In the present study, we demonstrated the potent apoptosis-inducing effect of Phx-3 on glioblastoma cell line LN229. We further investigated the effect of Phx-3 on ERK-Akt signaling and JNK signaling in order to clarify the molecular mechanism of its apoptosis induction.

Materials and methods

Materials. Phx-3 (Fig. 1) was prepared by reacting *o*-aminophenol with bovine erythrocyte suspension, following the method of Nakachi *et al* (17). Phx-3 was dissolved in a mixture of dimethylsulfoxide and ethyl alcohol (3:1) as a vehicle to make a 20-mM solution and was diluted appropriately with an isotonic saline for the experiments. Primary antibodies of phospho (p)-Akt, Akt, p-JNK, p-mTOR, mTOR and XIAP were purchased from Cell Signaling Technology (Beverly, MA, USA). Antibodies against p-ERK, ERK, JNK, PARP and GAPDH were purchased from Santa Cruz Biotechnology, Inc. (Santa Cruz, CA, USA). Anti-LC-3 monoclonal antibody (mAb) was obtained from Novus Biologicals (Littleton, CO, USA). A polyclonal antibody (Ab) against survivin, MP001, was prepared in our laboratory. Melatonin was purchased from Nakariai Tesque, Inc. (Kyoto, Japan) and N-acetyl-L-cysteine (NAC) was obtained from Sigma (St. Louis, MO, USA). U0126 and SP600125 were obtained from Merck KgaA (Darmstadt, Germany) and 5-(and-6)-chloromethyl-2', 7'-dichlorodihydrofluorescein diacetate (CM-H_2DCFDA) was obtained from Invitrogen (Carlsbad, CA, USA).

Cell culture and viability assay. Human glioblastoma cell line LN229 was cultured in Dulbecco's modified Eagle's medium (Sigma) supplemented with 10% heat-inactivated fetal calf serum (Equitech-Bio, Kerrville, TX, USA) at 37˚C in a 5% CO_2 humidified atmosphere. LN229 cells (3,000 cells/well) in 100 μl of culture medium were incubated with or without various concentrations of Phx-3 for 24-96 h in 96-well plates. The number of viable cells was assessed using a CellTiter-Blue Cell Viability Assay kit (Promega Co., Ltd., Madison, WI, USA), with fluorescence measurements at 570 nm for excitation and 590 nm for emission using a Powerscan HT Multidetection Microplate Reader (Dainippon Pharmaceutical, Osaka, Japan).

Cell morphology. The LN229 cells were plated in 24-well Ezview Glass Bottom Culture Plates (Iwaki, Asahi Techno Glass, Tokyo, Japan) at a density of $3x10^5$ cells/well and cultured for 24 h to completely attach them to the surface of the plates. The cells were treated with or without different concentrations of Phx-3 (2, 5 and 10 μM) in the presence or absence of 10 μM U0126, 10 μM SP600125, or 0.5 mM melatonin for 6 and 20 h. Morphological changes were examined by digital microscopy using BZ-8000 (Keyence Co., Osaka, Japan).

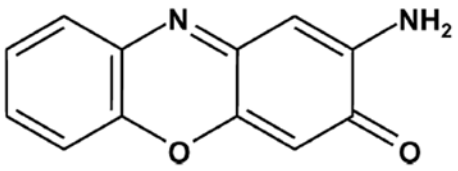

Figure 1. The chemical structure of Phx-3.

Apoptosis detection. Apoptotic cells were quantitatively evaluated by flow cytometry using an Annexin V-Fluorescein Staining kit (Wako Pure Chemical, Inc., Osaka, Japan). LN229 cells were treated with various concentrations of Phx-3 for the indicated time in the presence or absence of 10 μM U0126, 10 μM SP600125, or 0.5 mM melatonin. The cells were then harvested and stained with Annexin V and propidium iodide (PI). The levels of fluorescent staining of the cells were analyzed using a flow cytometer (Partec PAS; Partec, Münster, Germany) to estimate the population of apoptotic cells gated in Annexin V^+/PI^-, Annexin V^+/PI^+ and Annexin V^-/PI^+.

Immunoblotting. Immunoblotting was performed as previously described (18). Briefly, cells were lysed with RIPA lysis buffer (Nacalai Tesque, Inc., Kyoto, Japan) containing 1 mM PMSF, 0.15 U/ml aprotinin, 10 mM EDTA, 10 mg/ml sodium fluoride and 2 mM sodium orthovanadate. Cellular proteins were quantified using a Protein Assay Bicinchoninate kit (Nakalai Tesque, Inc.). Lysates containing 40 μg proteins were subjected to SDS-polyacrylamide gel electrophoresis (SDS-PAGE) and then transferred to an Immobilon-P membrane (Millipore, Bedford, MA). The membrane was incubated with primary Ab (dilution of 1:1,000) overnight at 4˚C. Immunoreactive proteins were detected with a horseradish peroxidase-conjugated secondary Ab and enhanced chemiluminescence reagent (ECL) (Millipore). Densitometry was performed using a Molecular Imager ChemiDoc XRS System (Bio-Rad).

Detection of intracellular ROS. Reactive oxygen species (ROS) production was determined using CM-H_2DCFDA, which diffuses through the cell membrane and is hydrolyzed by esterases to non-fluorescent dichlorofluorescein (DCFH) in cells. In the presence of ROS, this compound is oxidized to highly fluorescent dichlorofluorescein (DCF) in cells. For these experiments, LN229 cells were treated with or without Phx-3 (2, 5, or 10 μM) for 2.5 h at 37˚C in the presence or absence of 0.5 mM melatonin or 5 mM NAC. The cells were then incubated with 10 μM H_2DCFDA for an additional 30 min at 37˚C and trypsinized and washed with ice-cold phosphate buffered saline (PBS). Fluorescence was quantified using a flow cytometer Partec PAS (Partec).

Detection of mitochondrial membrane potential. Reduced mitochondrial membrane potential was monitored using a sensitive fluorescent dye, 5,5',6,6'-tetrachloro-1,1',3,3'-tetra-

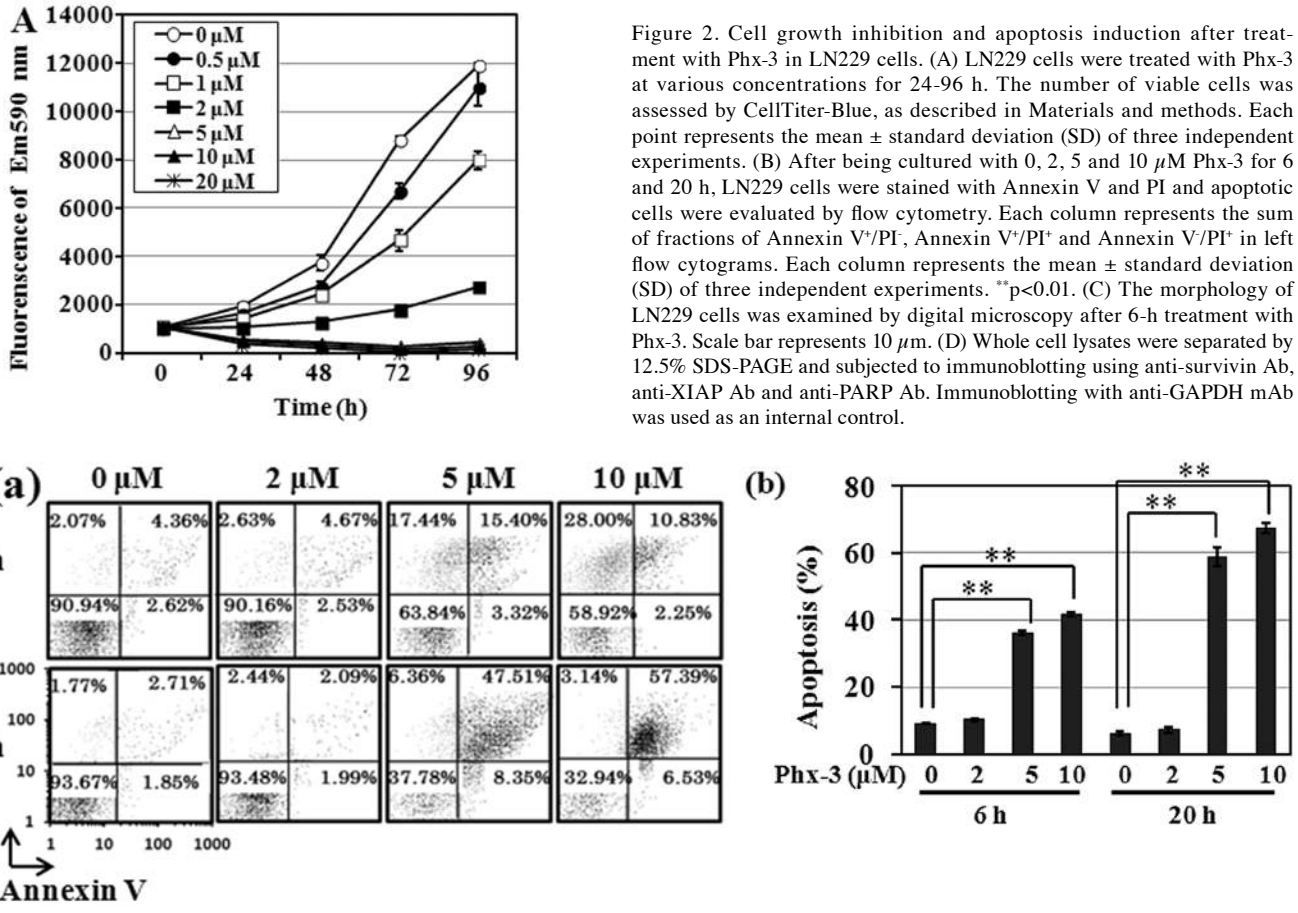

Figure 2. Cell growth inhibition and apoptosis induction after treatment with Phx-3 in LN229 cells. (A) LN229 cells were treated with Phx-3 at various concentrations for 24-96 h. The number of viable cells was assessed by CellTiter-Blue, as described in Materials and methods. Each point represents the mean ± standard deviation (SD) of three independent experiments. (B) After being cultured with 0, 2, 5 and 10 μM Phx-3 for 6 and 20 h, LN229 cells were stained with Annexin V and PI and apoptotic cells were evaluated by flow cytometry. Each column represents the sum of fractions of Annexin V^+/PI^-, Annexin V^+/PI^+ and Annexin V^-/PI^+ in left flow cytograms. Each column represents the mean ± standard deviation (SD) of three independent experiments. $^{**}p<0.01$. (C) The morphology of LN229 cells was examined by digital microscopy after 6-h treatment with Phx-3. Scale bar represents 10 μm. (D) Whole cell lysates were separated by 12.5% SDS-PAGE and subjected to immunoblotting using anti-survivin Ab, anti-XIAP Ab and anti-PARP Ab. Immunoblotting with anti-GAPDH mAb was used as an internal control.

ethylbenzimidazolylcarbocyanine iodide (JC-1) (Molecular Probes, Eugene, OR, USA) as previous described (10). Red fluorescence is attributed to potential-dependent aggregation in the mitochondria; green fluorescence, reflecting the monomeric form of JC-1, represents the dye in the cytosol after mitochondrial membrane depolarization. LN229 cells were treated with Phx-3 in the presence or absence of 10 μM of U0126 or SP600125, or 0.5 mM melatonin for 3 and 20 h. The cells were then stained with DMEM medium containing 5 μM JC-1 for 30 min at 37˚C. Relative fluorescence intensities were monitored by flow cytometry and instantly assessed for red and green fluorescence using a flow cytometer (Partec PAS; Partec).

Statistical analysis. All the quantitative data were expressed as mean ± standard deviation (SD). Student's t-test was used to compare the values for the population of apoptotic cells. A p-value of <0.05 was considered to be statistically significant.

Results

Phx-3 induces apoptosis in human glioblastoma cell line LN229. The growth of LN229 cells was significantly inhibited at 1 μM Phx-3 and was almost completely inhibited at >2 μM Phx-3 (Fig. 2A). The IC_{50} values (50% inhibition of cell growth) of Phx-3 on LN229 cells were 2.602±0.087 μM for 24 h and 1.655±0.093 μM for 48 h. These results indicated that

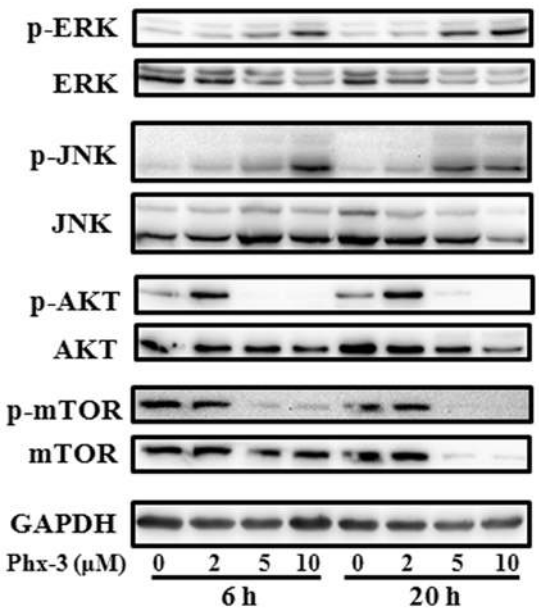

Figure 3. Expression and phosphorylation states of ERK, JNK, Akt and mTOR after treatment with Phx-3 in LN229 cells. After treatment with 0, 2, 5 and 10 μM Phx-3 for 6 and 20 h, LN229 cell lysates were subjected to 12.5% SDS-PAGE and immunoblotted with anti-p-JNK and JNK Abs, anti-p-ERK and anti-ERK Abs, anti-p-Akt and anti-Akt Abs and anti-p-mTOR and anti-mTOR Abs. Immunoblotting with anti-GAPDH mAb was used as an internal control.

Phx-3 exhibits a more potent cell growth inhibitory effect at a lower concentration in glioblastoma cell line LN229 than in other cell lines in our previous studies (8). We next examined apoptosis induction in LN229 cells treated with the indicated concentration of Phx-3 for 6 and 20 h (Fig. 2B). The population of apoptotic cells [Annexin V(+)/PI(-) + Annexin V(+)/PI(+) + Annexin V(-)/PI(+)] induced by Phx-3 increased in a dose- and a time-dependent manner. The characteristics of apoptotic morphology (e.g., cytoplasm shrinking, plasma membrane blebbing and nuclear condensation) were observed (Fig. 2C).

We next investigated the expression profiles of survivin, XIAP and poly (ADP-ribose) polymerase (PARP). Survivin and XIAP, members of the inhibition of apoptosis (IAP) family, suppress cell death by inhibiting the caspase family. PARP, which is the substrate of caspase-3, is cleaved during drug-induced apoptosis. Expressions of survivin and XIAP decreased after treatment with Phx-3 in a time- and dose-dependent manner (Fig. 2D). Although cleaved PARP was not clear, the 114 KDa of PARP expressions significantly decreased after treatment with Phx-3.

JNK activation is the main pathway of Phx-3-induced apoptosis. Both the suppression of survival signaling and the activation of apoptotic signaling could induce apoptosis. The Akt and ERK signaling pathway plays a key role in cell proliferation, survival and differentiation (14,15), whereas the activation of JNK pathways is involved in pro-apoptotic signaling in response to various chemical and environmental stresses (16). In order to clarify the molecular mechanisms of Phx-3-induced apoptosis in LN229 cells, we focus on the ERK-Akt and the JNK signaling pathways. The level of p-ERK and p-JNK significantly increased after treatment with Phx-3 for 6 h and was sustained for ≥20 h (Fig. 3). Conversely, the phosphorylation levels of Akt and mTOR, a downstream target of Akt, were suppressed after treatment with Phx-3. These results suggest that activation of ERK and JNK, as well as suppression of Akt and mTOR, might contribute to apoptosis induction by Phx-3.

To investigate whether ERK plays an important role in apoptosis induction by Phx-3, we treated the cells with Phx-3 in the presence or absence of ERK inhibitor U0126 for 6 and 20 h; and apoptosis induction was assessed by flow cytometry. Although the phosphorylation of ERK induced by Phx-3 was almost completely suppressed in the presence of U0126 (Fig. 4A), Phx-3-induced apoptosis was only partially blocked (Fig. 4B and C). This result indicated that the ERK-Akt axis does not appear to be the major pathway for apoptosis induction. In addition, the suppression of Akt, but not mTOR was almost completely restored by U0126, which suggesting that Akt acts on downstream ERK signaling.

We next investigated the role of JNK activation. Activation of JNK in response to Phx-3 was repressed in the presence of 10 μM SP600125, a specific JNK inhibitor (Fig. 5A). It was noteworthy that, unlike U0126, the apoptosis induced by Phx-3 was almost completely blocked in the presence of SP600125 (Fig. 5B and C). Furthermore, the activation of ERK and the suppression of Akt were almost completely restored, while repression of survivin and XIAP and suppression of mTOR phosphorylation were still detectable (Fig. 5D and E). These results indicated that activation of JNK plays a critical role in apoptosis induction by Phx-3 in LN229 cells. In addition, JNK appears to localize upstream of ERK/Akt signaling.

JNK activation depends on Phx-3-induced ROS generation. The next question was how JNK was activated after treatment with Phx-3. In our previous study, we found that treatment of the lung adenocarcinoma cell line A549 with Phx-3 resulted in localization of Phx-3 in mitochondria along with ROS generation (10). Other studies indicated that suppression of JNK significantly protected against apoptosis induction by ROS (19). We therefore postulated that ROS generation might be involved in the activation of JNK in response to Phx-3. We first examined ROS generation in LN229 cells by measuring the fluorescence of H_2DCFDA. Fluorescence increased after 3-h exposure to Phx-3 in a dose-dependent manner (Fig. 6A). ROS production was significantly inhibited in the presence of 0.5 mM melatonin or 5 mM NAC, both of which are ROS scavengers. Melatonin inhibits ROS more strongly than NAC, so we used melatonin for the following studies. Notably, the presence of 0.5 mM melatonin at 6 and 20 h almost completely prevented apoptosis induction by Phx-3 (Fig. 6B and C). These results indicated that ROS generation in response to Phx-3 was strongly involved in apoptosis induction in LN229 cells. After elimination of ROS with melatonin treatment, Phx-3-induced JNK activation was also inhibited (Fig. 6E). As well as SP600125 treatment (Fig. 5E), melatonin also suppressed ERK phosphorylation and restored the phosphorylation state of Akt without any effect on the repression of survivin and XIAP, as well as suppression of mTOR phosphorylation (Fig. 6D and E). These results suggest that ROS generated by Phx-3 plays a pivotal role in apoptosis induction and JNK activation in LN229 cells.

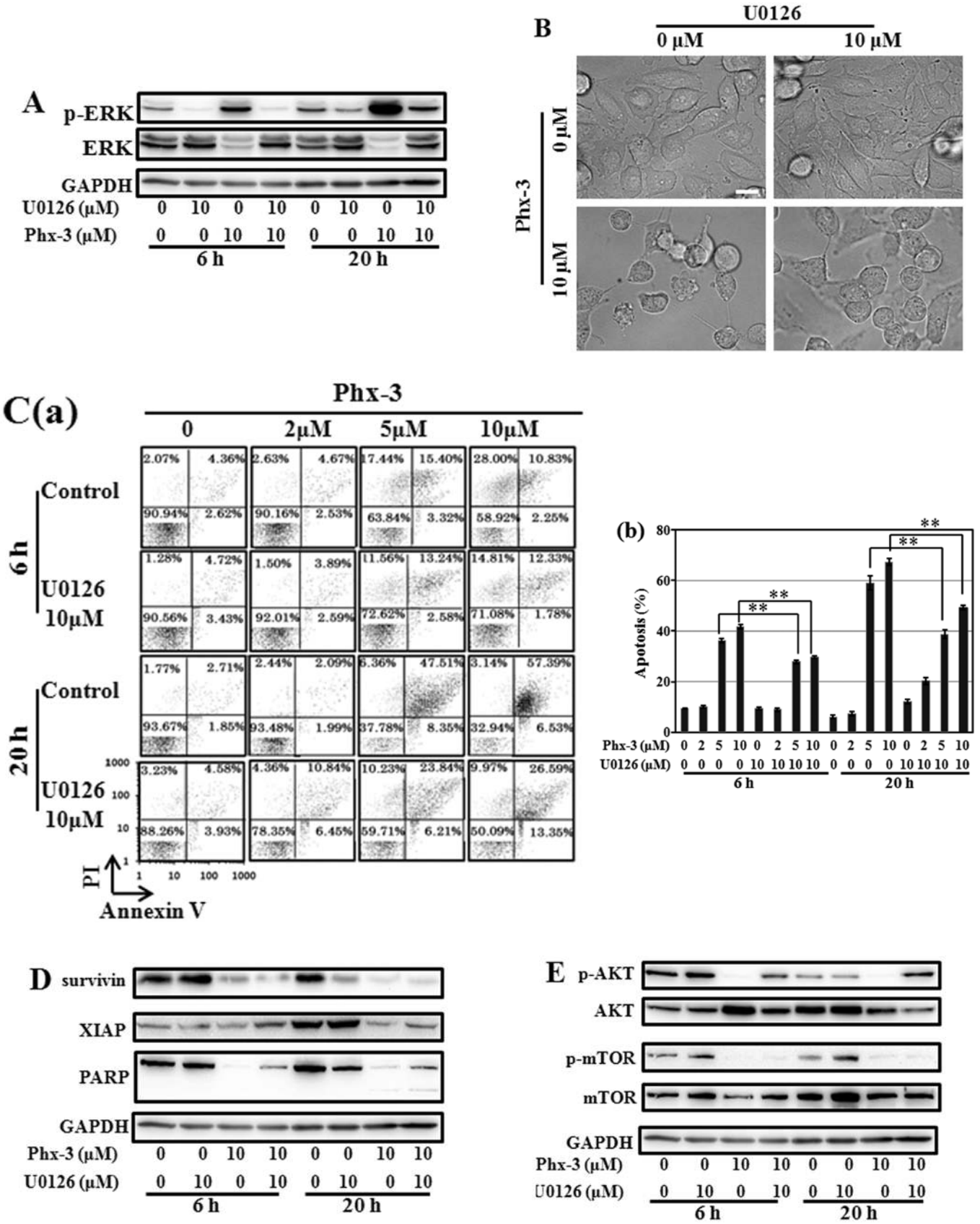

Figure 4. Role of JNK activation in apoptosis induction by Phx-3 in LN229 cells. (A) LN229 cells were treated with 0 or 10 μM Phx-3 in the presence or absence of 10 μM SP600125 for 6 and 20 h. The expression levels of p-JNK and JNK were then detected by immunoblotting. Immunoblotting with anti-GAPDH mAb was used as an internal control. (B) The morphology of LN229 cells was examined by digital microscopy after treatment with Phx-3 for 6 h. Scale bar represents 10 μm. (C) Cell apoptosis was assessed by flow cytometry. Each column represents the sum of fractions of Annexin V^+/PI^-, Annexin V^+/PI^+ and Annexin V^-/PI^+ in left flow cytograms. Each column represents the mean ± standard deviation (SD) of three independent experiments. $^{**}p<0.01$. (D) After treatment of Phx-3 in the presence or absence of SP600125, changes in the expression of survivin, XIAP and PARP were detected by immunoblotting. The expression level of GAPDH was used as an internal control. (E) The expression levels of p-ERK and ERK, p-Akt and Akt and p-mTOR and mTOR were detected by immunoblotting. Immunoblotting with anti-GAPDH mAb was used as an internal control.

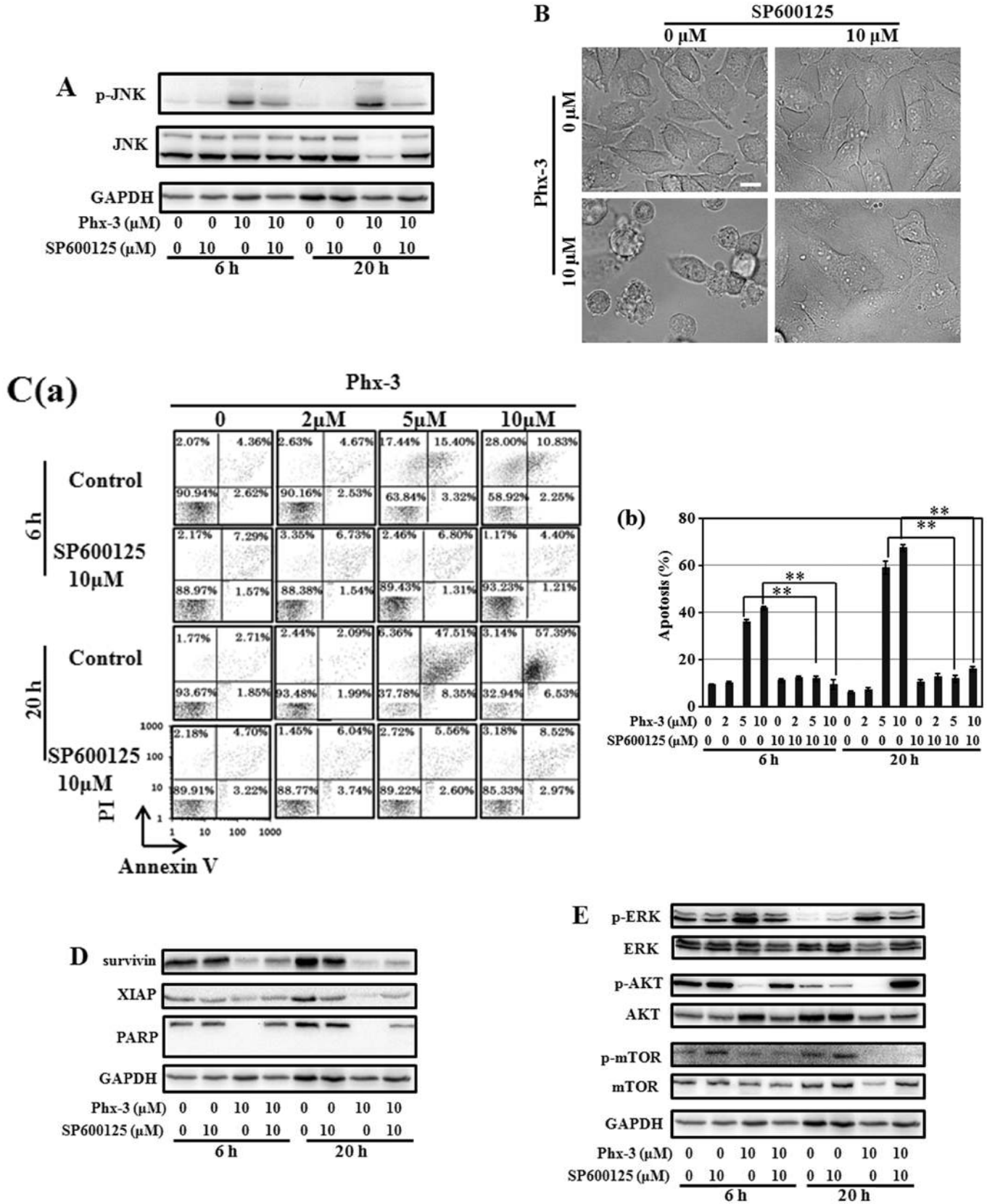

Figure 5. Role of ERK activation in apoptosis induction by Phx-3 in LN229 cells. (A) LN229 cells were treated with 0 or 10 μM Phx-3 in the presence or absence of 10 μM U0126, an ERK inhibitor, for 6 and 20 h. The cell lysates were then subjected to 12.5% SDS-PAGE and immunoblotted with anti-p-ERK and anti-ERK Ab. Immunoblotting with anti-GAPDH mAb was used as an internal control. (B) The cell morphology of LN229 cells was examined by digital microscopy after treatment with Phx-3 for 6 h. Scale bar represents 10 μm. (C) After treatment with 0 or 10 μM Phx-3 in the presence or absence of 10 μM U0126, apoptosis in LN229 cells was assessed by flow cytometry. Each column represents the sum of fractions of Annexin V^+/PI^-, Annexin V^+/PI^+ and Annexin V^-/PI^+ in left flow cytograms. Each column represents the mean ± standard deviation (SD) of three independent experiments. $^{**}p<0.01$. (D) After treatment with 0 or 10 μM Phx-3 in the presence or absence of 10 μM U0126, the expressions of survivin, XIAP and PARP were detected by immunoblotting. The expression of GAPDH was used as an internal control. (E) Immunoblot analysis of the changes in expression levels of p-Akt and Akt and p-mTOR and mTOR in LN229 cells treated with or without 10 μM Phx-3 in the presence or absence of 10 μM U0126. Immunoblotting with anti-GAPDH mAb was used as an internal control.

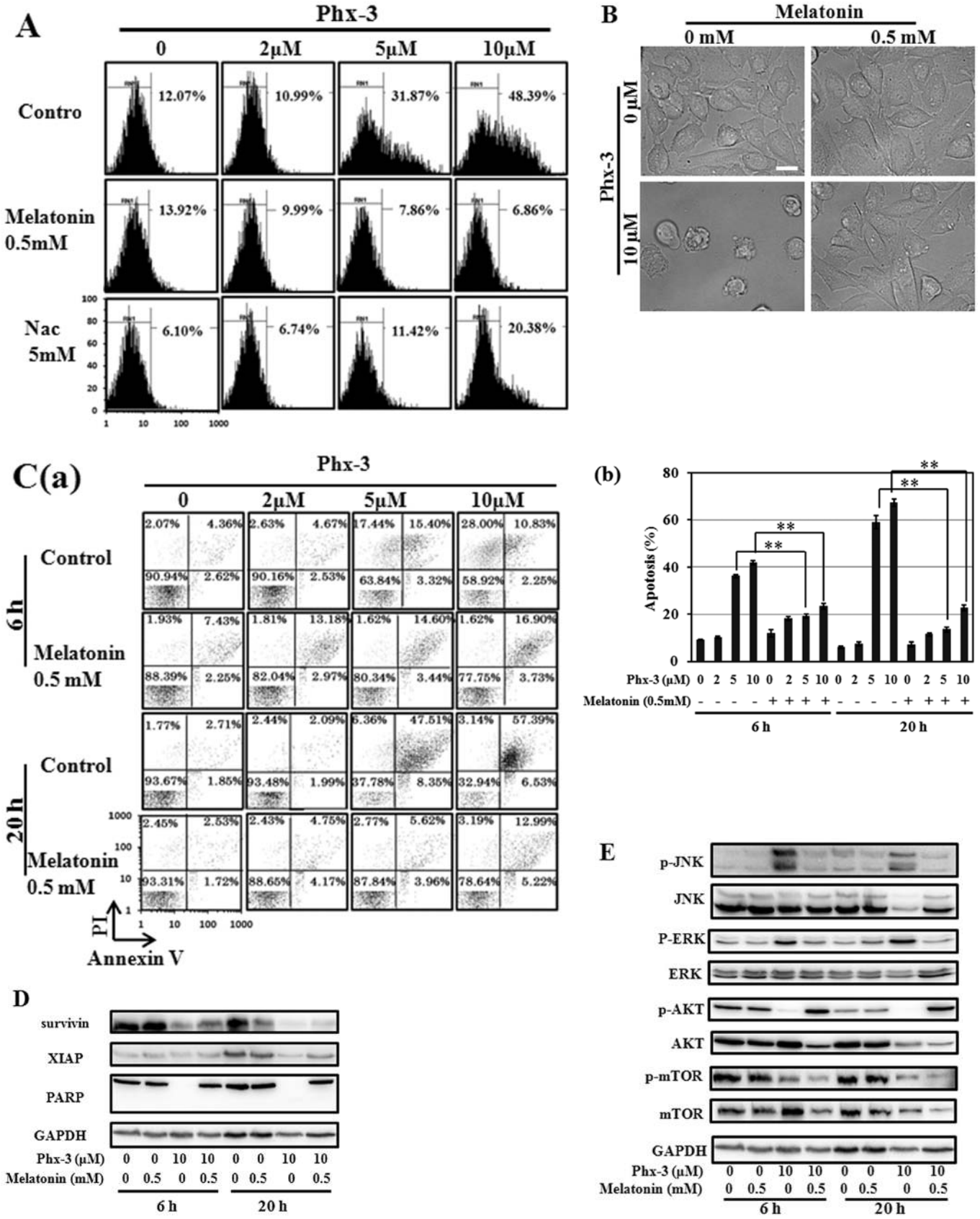

Figure 6. JNK activation mediated through Phx-3-induced ROS generation in LN229 cells. (A) LN229 cells were treated with 0, 2, 5 and 10 μM Phx-3 with or without 0.5 mM melatonin or 5 mM NAC for 2.5 h. The cells were then further incubated with H_2DCFDA for 30 min and ROS generation was assessed by flow cytometry. (B) After treatment with or without 10 μM Phx-3 in the presence or absence of 0.5 mM melatonin for 6 h, the morphology of LN229 cells was examined using digital microscopy. Scale bar represents 10 μm. (C) LN229 cells were treated with or without Phx-3 (2, 5 and 10 μM) in the presence or absence of 0.5 mM melatonin and cell apoptosis was assessed by flow cytometry. Each column represents the sum of fractions of Annexin V^+/PI^-, Annexin V^+/PI^+ and Annexin V^-/PI^+ in the left flow cytograms. Each column represents the mean ± standard deviation (SD) of three independent experiments. $^{**}p<0.01$. (D) Immunoblottings for the expression of survivin, XIAP and PARP. Immunoblotting with anti-GAPDH mAb was used as an internal control. (E) Changes in expression levels of p-JNK and JNK, p-ERK and ERK, p-Akt and Akt and p-mTOR and mTOR by immunoblotting. Immunoblotting with anti-GAPDH mAb was used as an internal control.

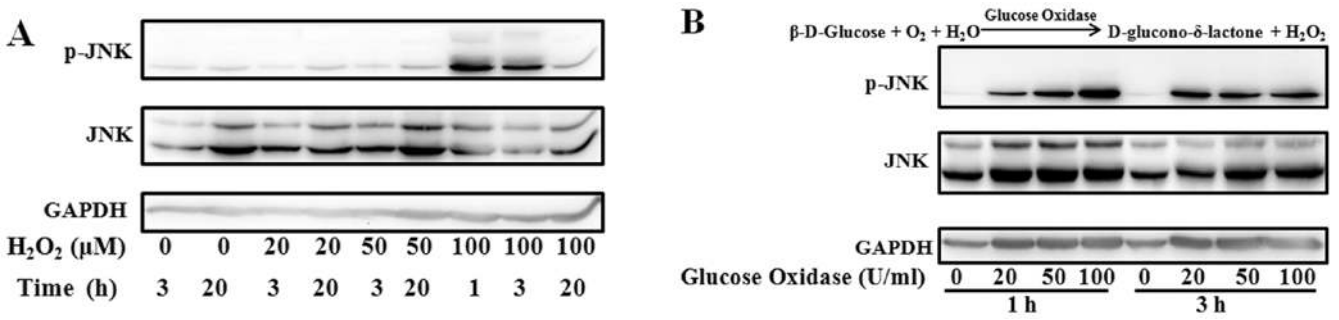

Figure 7. JNK activation by exogenous ROS in LN229 cells. (A) LN229 cells were cultured with or without H_2O_2 (20, 50 and 100 μM) for 1, 3 and 20 h. The expression levels of p-JNK and JNK were then examined by immunoblot analysis. Immunoblotting with anti-GAPDH mAb was used as an internal control. (B) LN229 cells were cultured with or without glucose oxidase (20, 50 and 100 U/ml), which could continuously catalyze glucose in the medium to hydrogen peroxide. Expressions of p-JNK and JNK were examined by immunoblot analysis after 1-, 3- and 20-h treatment with glucose oxidase. Immunoblotting with anti-GAPDH mAb was used as an internal control.

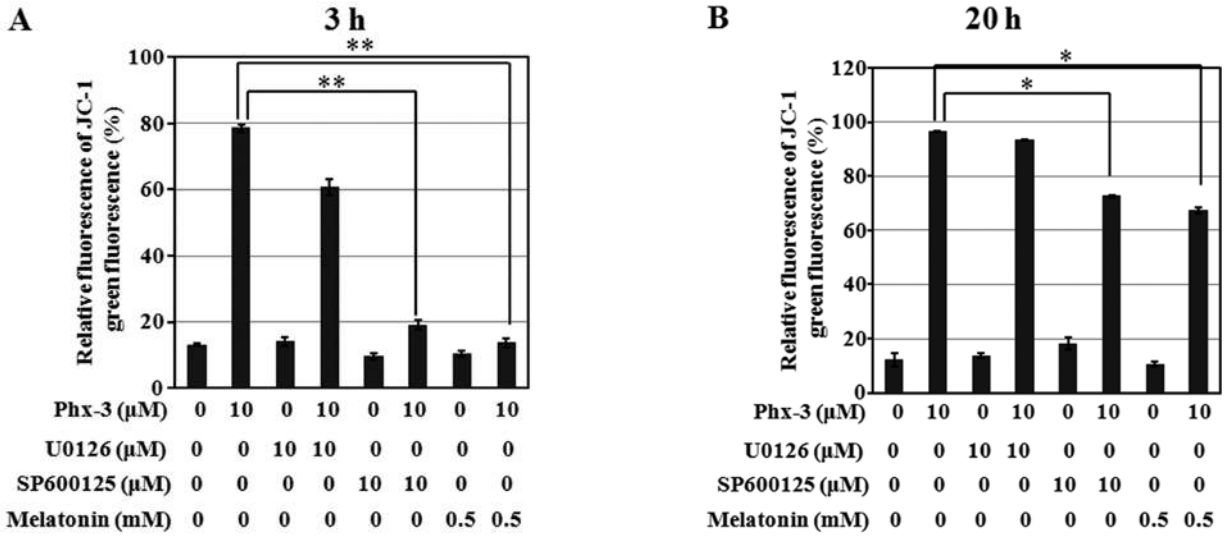

Figure 8. Depolarization of the mitochondrial membrane potential in LN229 cells. LN229 cells were treated with Phx-3 in the presence or absence of 10 μM of U0126, 10 μM SP600125, or 0.5 mM of melatonin for 3 h (A) or 20 h (B). Depolarization of the mitochondrial membrane potential was analyzed using flow cytometry. Each column represents the mean ± standard deviation (SD) of three independent experiments. $^{*}p<0.05$; $^{**}p<0.01$.

To confirm that ROS is the direct activator of JNK, we treated LN229 cells with various concentrations of H_2O_2 for 1-20 h (Fig. 7A). The results indicated that JNK phosphorylation increased transiently after treatment with 100 μM H_2O_2. Also, glucose oxidase catalyzes the oxidation of glucose to hydrogen peroxide and D-glucono-δ-lactone. With the addition of glucose oxidase to LN229 cell culture, the glucose in the medium should be continuously metabolized to hydrogen peroxide. The level of phospho-JNK increased in the presence of glucose oxidase (Fig. 7B). Therefore, ROS is the direct activator of JNK in LN229 cells.

JNK activation by ROS is involved in depolarization of the mitochondrial membrane. Mitochondria are considered the main source of ROS (20). Conversely, continuous ROS generation by mitochondria also causes the dysfunction of mitochondria (21). In addition, JNK translocates into the mitochondria, inactivates Bcl-2 and Bcl-xL and decreases the mitochondrial membrane potential, which leads to the activation of caspase cascade. We examined mitochondrial depolarization by JC-1 staining to evaluate the mitochondrial membrane integrity after treatment with Phx-3 in the presence or absence of U0126, SP600125 and melatonin. In intact cells, JC-1 accumulates in mitochondria and emits primarily red fluorescence; in the mitochondrial depolarized cells, JC-1 emits green fluorescence when leaking from mitochondria to cytoplasm. Relative green fluorescence significantly increased in the cells treated with 10 μM Phx-3 for 3 h (Fig. 8A). This depolarization was blocked in the presence of either SP600125 or melatonin, but not in the presence of U0126. However, with exposure time extended to 20 h (Fig. 8B), mitochondrial depolarization was only slightly blocked even in the presence of SP600125 or melatonin. Therefore, sustained mitochondrial dysfunction by some alternative mechanism(s) may cause apoptosis even if the cells are treated with JNK inhibitor or ROS scavenger.

All the data above suggest that for short-time exposure to Phx-3, ROS generation, followed by JNK activation is the main axis for apoptosis induction in response to Phx-3. However, for longer exposure to Phx-3, mitochondrial dysfunction may cause other apoptotic machinery in LN229 cells.

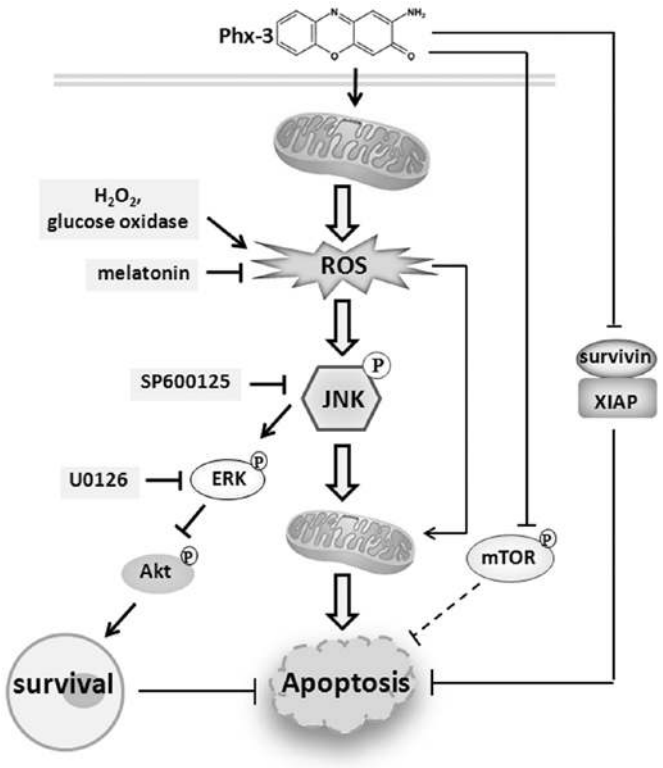

Figure 9. Scheme of apoptosis pathways induced by Phx-3. Multiple pathways are involved in Phx-3-induced apoptosis. The pivotal pathway is mediated through ROS production following JNK activation. Phx-3 downregulates the expression of survivin and XIAP independent of the ROS/JNK pathway. Sustained depolarization of mitochondrial potential in response to >20-h exposure to Phx-3 appears to be involved in apoptosis induction. Additionally, the suppression of mTOR by Phx-3 may be related to Phx3-induced apoptosis.

Discussion

In the present study, we found that the oxidative form of Phx-3 potently induced apoptosis in the glioblastoma cell line LN229 (Fig. 2). In addition, we confirmed that the ROS/JNK axis is the pivotal pathway for apoptosis induction. This conclusion is supported by the following results (1). Phx-3 induced concomitant activation of both JNK and ERK pathways; however, JNK inhibitor SP600125 completely blocked apoptosis induction by Phx-3, but ERK inhibitor U0126 did not (Figs. 4 and 5) (2). Phx-3 treatment induced ROS generation within 3 h (Fig. 6A); however, the ROS scavenger melatonin almost completely blocked Phx-3-induced apoptosis and JNK activation (Fig. 6B, C and E) (3). Exogenous ROS generation with the addition of H_2O_2 or glucose oxidase in culture medium resulted in JNK activation (Fig. 7).

Cellular endogenous ROS is implicated in genotoxicity, tumor initiation and progression and a high level of ROS induces cell death via apoptotic and/or necrotic mechanisms (22). In addition to Phx-3, the anticancer agents that are generally used (e.g., cisplatin, vinblastine and doxorubicin) exert their pharmacological effects through ROS-mediated cell death induction (21). Mitochondria are the main source of endogenous ROS and antioxidant systems such as superoxide dismutase (SOD) and glutathione peroxidase (GPx) eliminate over-generated ROS, keeping the cells in homeostasis (23). Therefore, either exogenous ROS production or inhibition of the antioxidant systems induces an accumulation of cellular ROS. In this study, significant increase of ROS generation (Fig. 6A) and dramatic decrease of mitochondrial membrane potential (Fig. 8A) were detected after 3-h treatment with Phx-3. In our previous study, microscopic examination indicated that Phx-3 localized mainly in the mitochondria within 1-h exposure in A549 cells, a lung adenocarcinoma cell line and ROS generation induced by Phx-3 contributed to apoptosis induction (10). Therefore, mitochondria appear to be the direct target of Phx-3 and overwhelming ROS generation by mitochondria appears to be involved in apoptotic induction.

Several signaling pathways (e.g., ERK, JNK and p38 kinases) are activated in response to ROS generation (24-26). In response to DNA damage by ROS, sustained activation of both JNK and ERK mediates cell death (24,25). As well as these previous reports, JNK and ERK were activated after treatment with Phx-3 in LN229 cells (Fig. 3) and their activation was concomitantly blocked in the presence of melatonin, a ROS scavenger, along with inhibition of Phx-3-induced apoptosis (Fig. 6E). We analyzed which signal is critical for Phx-3-induced apoptosis and found that apoptosis induction by Phx-3 was completely blocked by SP600125, a specific inhibitor of JNK. However, U0126, an inhibitor of ERK, only partially suppressed apoptosis induction (Figs. 4C and 5C). This result indicates that activation of JNK mediated through ROS generation is the main pathway of Phx-3-induced apoptosis. Additionally, treatment with SP600125 inhibited ERK activation (Fig. 5E), which suggests that ERK is located on one of the downstream pathways of JNK.

The molecular mechanism of JNK activation in response to ROS is still unclear in our system. It has been reported that signaling pathways such as ASK1 (27,28), Src kinase (29) and glutathione S-transferase Pi (GSTπ) (30,31) are involved in ROS-mediated JNK activation. In the presence of ROS, oxidized thioredoxin and/or glutaredoxin, which is dissociated from ASK1, resulted in activation of ASK1 followed by subsequent JNK phosphorylation (27,28). Src kinase is also reported to be an important redox-sensitive pathway for JNK activation after treatment with H_2O_2 (29). Additionally, the monomeric form of GSTπ suppresses JNK activity (30), while the oligomeric form of GSTπ induced by H_2O_2 treatment activates JNK (31). Further studies are required to clarify the pathway from ROS to JNK activation after Phx-3 treatment.

It is noteworthy that SP600125 and melatonin did not suppress the depolarization of mitochondria after 20-h treatment with Phx-3, although these reagents blocked Phx-3-induced apoptosis (Fig. 8B). When Phx-3 exposure time was extended to 72 h, apoptosis in LN229 cells was detectable even in the presence of SP600125 or melatonin (data not shown). These results suggest that the ROS/JNK pathway is indeed the main axis for apoptosis induction during short-time exposure to Phx-3, however, with longer exposure, some alternative mechanism(s) causing irreversible mitochondrial demoralization may be involved in apoptosis induction. Phx-3-induced suppression of mTOR activity and downregulation of survivin and XIAP may also be involved in these alternative mechanisms. These molecules were not restored in the presence of U0126, SP600125, or melatonin (Figs. 4D and E, 5D and E and 6D and E), so they are considered to be independent of the ROS/JNK axis. However, Phx-3 efficiently inhibited Akt

activation and this inhibition was completely restored in the presence of U0126, as well as SP600125 and melatonin. This result suggests that Akt is located downstream of ERK. Sinha *et al* reported that withdrawal of survival factors leads to activation of ERK and suppression of Akt activity, along with apoptosis induction in mouse renal proximal tubular cells (32). This apoptosis was inhibited by U0126 or PD98059, indicating that ERK plays a role in suppressing survival signaling through decreasing Akt activity (32). Similarly, U0126 partially blocked the apoptosis induced by Phx-3 (Fig. 5B and C), suggesting that the suppression of Akt might partially promote cell death in our system during exposure to Phx-3. However, the Phx-3-induced inhibition of mTOR, which is a key molecule of Akt signaling, was not restored when Akt activation was restored in the presence of melatonin, SP600125, or U0126 (Figs. 4E, 5E and 6E). Therefore, the inhibition of mTOR by Phx-3 may be mediated through the Akt-independent pathway.

Collectively, Phx-3 appears to induce apoptosis through multiple pathways (Fig. 9). In 20-h exposure to Phx-3, ROS/JNK signaling is the pivotal pathway for apoptosis induction. However, with longer exposure, some alternative mechanism(s) causing irreversible mitochondrial demoralization may also be involved in apoptosis induction. Therefore, if the cells have any functional defects in the pathway from ROS to JNK, some alternate mechanisms (e.g., downregulation of survivin and XIAP, or inhibition of mTOR activity) may be involved in apoptosis induction. Phenoxazine derivatives are able to pass through the blood-brain barrier (11), so our findings suggest that Phx-3 has high potential as an anticancer reagent for glioblastoma therapy.

Acknowledgements

This study was supported by funds from the Private University Strategic Research-Based Support Project (Molecular Information-based Intractable Disease Research Project) from the Ministry of Education, Culture, Sports, Science and Technology of Japan to A.T. and K.M. (2008-2012), and a Grant-in-Aid from the Tokyo Medical University for Cancer Research to X.C., Japan.

References

1. Bidros DS and Vogelbaum MA: Novel drug delivery strategies in neuro-oncology. Neurotherapeutics 6: 539-546, 2009.
2. Tomoda A, Arai S, Ishida R, Shimamoto T and Ohyashiki K: An improved method for the rapid preparation of 2-amino-4,4·-dihydro-4·,7-dimethyl-3Hphenoxazine-3-one, a novel antitumor agent. Bioorg Med Chem Lett 11: 1057-1058, 2001.
3. Shimizu S, Suzuki M, Tomoda A, Arai S, Taguchi H, Hanawa T and Kamiya S: Phenoxazine compounds produced by the reactions with bovine hemoglobin show antimicrobial activity against non-tuberculosis mycobacteria. Tohoku J Exp Med 203: 47-52, 2004.
4. Shimamoto T, Tomoda A, Ishida R and Ohyashiki K: Antitumor effects of a novel phenoxazine derivative on human leukemia cell lines in vitro and in vivo. Clin Cancer Res 7: 704-708, 2001.
5. Shirato K, Imaizumi K, Miyazawa K, Takasaki A, Mizuguchi J, Che XF, Akiyama S and Tomoda A: Apoptosis induction preceded by mitochondrial depolarization in multiple myeloma cell line U266 by 2-aminophenoxazine-3-one. Biol Pharm Bull 31: 62-67, 2008.
6. Shirato K, Imaizumi K, Abe A and Tomoda A: Phenoxazine derivatives induce caspase-independent cell death in human glioblastoma cell lines, A-172 and U-251MG. Oncol Rep 17: 201-208, 2007.
7. Miyano-Kurosaki N, Kurosaki K, Hayaashi M, Takaku H, Hayafune M, Shrato K, Kasuga T, Endo T and Tomoda A: 2-Aminophenoxazine-3-one suppresses the growth of mouse malignant melanoma B16 cells transplanted into C57BL/6Cr Slc mice. Biol Pharm Bull 29: 2197-2201, 2006.
8. Che XF, Zheng CL, Akiyama S and Tomoda A: 2-Amino phenoxazine-3-one and 2-amino-4,4α-dihydro-4α,7-dimethyl-3H-phenoxazine-3-one cause cellular apoptosis by reducing higher intracellular pH in cancer cells. Proc Jpn Acad Ser B Phys Biol Sci 87: 199-213, 2011.
9. Takasaki A, Hanyu H, Iwamoto T, Shirato K, Izumi R, Toyota H, Izuguchi J, Miyazawa K and Tomoda A: Mitochondrial depolarization and apoptosis associated with sustained activation of c-jun-N-terminal kinasein the human multiple myeloma cell line U266 induced by 2-aminophenoxazine-3-one. Mol Med Rep 2: 199-203, 2009.
10. Zheng CL, Che XF, Akiyama S, Miyazawa K and Tomoda A: 2-Aminophenoxazine-3-one induces cellular apoptosis by causing rapid intracellular acidification and generating reactive oxygen species in human lung adenocarcinoma cells. Int J Oncol 36: 641-650, 2010.
11. Azuine MA, Tokuda H, Takayasu J, Enjyo F, Mukainaka T, Konoshima T, Nishino H and Kapadia GJ: Cancer chemopreventive effect of phenothiazines and related tri-heterocyclic analogues in the 12-O-tetradecanoylphorbol-13-acetate promoted Epstein-Barr virus early antigen activation and the mouse skin two-stage carcinogenesis models. Pharmacol Res 49: 161-169, 2004.
12. Nakada M, Kita D, Watanabe T, Hayashi Y, Teng L, Pyko IV and Hamada J: Aberrant signaling pathways in glioma. Cancers 3: 3242-3278, 2011.
13. Soni D, King JA, Kaye AH and Hovens CM: Genetics of glioblastoma multiforme: mitogenic signaling and cell cycle pathways converge. J Clin Neurosci 12: 1-5, 2005.
14. Los M, Maddika S, Erb B and Schulze-Osthoff K: Switching Akt: from survival signaling to deadly response. Bioessays 31: 492-495, 2009.
15. Pearson G, Robinson F, Beers Gibson T, Xu BE, Karandikar M, Berman K and Cobb MH: Mitogen-activated protein (MAP) kinase pathways: regulation and physiological functions. Endocr Rev 22: 153-183, 2001.
16. Davis RJ: Signal transduction by the JNK group of MAP kinases. Cell 103: 239-252, 2000.
17. Nakachi T, Tabuchi T, Takasaki A, Arai S, Miyazawa K and Tomoda A: Anticancer activity of phenoxazines produced by bovine erythrocytes on colon cancer cells. Oncol Rep 23: 1517-1522, 2010.
18. Kawaguchi T, Miyazawa K, Moriya S, Ohtomo T, Che XF, Naito M, Itoh M and Tomoda A: Combined treatment with bortezomib plus bafilomycin A1 enhances the cytocidal effect and induces endoplasmic reticulum stress in U266 myeloma cells: crosstalk among proteasome, autophagy-lysosome and ER stress. Int J Oncol 38: 643-654, 2011.
19. Nohl H, Gille L and Staniek K: Intracellular generation of reactive oxygen species by mitochondria. Biochem Pharmacol 69: 719-723, 2005.
20. Gogvadze V, Orrenius S and Zhivotovsky B: Mitochondria as targets for cancer chemotherapy. Semin Cancer Biol 19: 57-66, 2009.
21. Maundrell K, Antonsson B, Magnenat E, Camps M, Muda M, Chabert C, Gillieron C, Boschert U, Vial-Knecht E, Martinou JC and Arkinstall S: Bcl-2 undergoes phosphorylation by c-Jun N-terminal kinase/stress-activated protein kinases in the presence of the constitutively active GTP-binding protein Rac1. J Biol Chem 272: 25238-25242, 1997.
22. Basu A and Haldar S: Identification of a novel Bcl-xL phosphorylation site regulating the sensitivity of taxol- or 2-methoxyestradiol-induced apoptosis. FEBS Lett 538: 41-47, 2003.
23. Fulda S, Gorman AM, Hori O and Samali A: Cellular stress responses: cell survival and cell death. Int J Cell Biol 2010: 214074, 2010.
24. Trachootham D, Lu W, Ogasawara MA, Valle NR and Huang P: Redox regulation of cell survival. Antioxid Redox Signal 10: 1343-1374, 2008.
25. Feligioni M, Brambilla E, Camassa A, Sclip A, Arnaboldi A, Morelli F, Antoniou X and Borsello T: Crosstalk between JNK and SUMO signaling pathways: deSUMOylation is protective against H_2O_2-induced cell injury. PLoS One 6: e28185, 2011.

26. Conde de la Rosa L, Schoemaker MH, Vrenken TE, Buist-Homan M, Havinga R, Jansen PL and Moshage H: Superoxide anions and hydrogen peroxide induce hepatocyte death by different mechanisms: involvement of JNK and ERK MAP kinases. J Hepatol 44: 918-929, 2006.
27. Matos TJ, Duarte CB, Goncalo M and Lopes MC: Role of oxidative stress in ERK and p38 MAPK activation induced by the chemical sensitizer DNFB in a fetal skin dendritic cell line. Immunol Cell Biol 83: 607-614, 2005.
28. Tobiume K, Matsuzawa A, Takahashi T, Nishitoh H, Morita K, Takeda K, Minowa O, Miyazono K, Noda T and Ichijo H: ASK1 is required for sustained activations of JNK/p38 MAP kinases and apoptosis. EMBO Rep 2: 222-228, 2001.
29. Song JJ, Rhee JG, Suntharalingam M, Walsh SA, Spitz DR and Lee YJ: Role of glutaredoxin in metabolic oxidative stress: glutaredoxin as a sensor of oxidative stress mediated by H_2O_2. J Biol Chem 277: 46566-46575, 2002.
30. Yoshizumi M, Abe J, Haendeler J, Huang Q and Berk BC: Src and Cas mediate JNK activation but not ERK1/2 and p38 kinases by reactive oxygen species. J Biol Chem 275: 11706-11712, 2000.
31. Wang T, Arifoglu P, Ronai Z and Tew KD: Glutathione S-transferase P1-1 (GSTP1-1) inhibits c-Jun N-terminal kinase (JNK1) signaling through interaction with the C terminus. J Biol Chem 276: 20999-21003, 2001.
32. Sinha D, Bannergee S, Schwartz JH, Lieberthal W and Levine JS: Inhibition of ligand-independent ERK1/2 activity in kidney proximal tubular cells deprived of soluble survival factors upregulates Akt and prevents apoptosis. J Biol Chem 279: 10962-10972, 2004.